

ARTICLES

Formation and Valence Band Density of States of Nonspherical Cu Nanoparticles Deposited on Si(100) Substrate**Z. Pászti,* G. Pető, Z. E. Horváth, and A. Karacs***Research Institute for Materials Science, Central Research Institute for Physics, P.O. Box 49, Budapest, Hungary H-1525***L. Guzzi***Department of Surface Chemistry and Catalysis, Institute of Isotopes, P.O. Box 77, Budapest, Hungary H-1525**Received: May 22, 1996; In Final Form: December 3, 1996*[®]

Copper thin films consisting of nanosized particles were deposited on a Si(100) single-crystal substrate by laser ablation in an argon atmosphere. In order to obtain isolated particles with nanometer sizes, the film was sputtered by low-energy Ar⁺ ions. The valence band density of states of the film was in situ investigated by X-ray and ultraviolet photoelectron spectroscopies (XPS and UPS) during the Ar⁺ ion sputtering. The size of the particles formed after sputtering was in the range between 3 and 6 nm in lateral dimension and 2–3 nm in height, as measured by transmission electron microscopy. In the as-deposited state the photoelectron spectrum of the thin layer was identical to what was observed in the bulk. At the end of thinning by Ar⁺ ion sputtering the 3d valence states were rehybridized with respect to the bulk states, which indicates that the lower binding energy part of the d band (around 2.5 eV) is the most sensitive for size reduction. The Fermi edge became undetectable by photoemission. These data show that the valence band of small particles are affected by both the size and geometry of the particles. Supporting experiments showed that the effect is attributed to neither copper silicide formation nor intermixing.

Introduction

Investigation of small metallic particles is a very active area in solid state physics and chemistry. Studies on these systems provide information about the development of the electronic structure of materials in the size range between isolated atom and bulk solid. Knowledge of size dependence of the electronic structure is very important for understanding the enhanced catalytic activity and the special magnetic properties observed in small particles.

Until now, the majority of publications have dealt with small particles deposited onto different substrates.^{1–16} In those experiments different transition and noble metals were deposited on carbon, metaloxide, or silicon oxide substrates by thermal or electron beam evaporation in a very thin layer. It was assumed that on these substrates the metal deposit forms evenly spaced, isolated 3-dimensional islands. The size of the islands (small particles) was estimated from the coverage of the substrate. The main tool of investigation was photoelectron spectroscopy (partly UPS and mainly XPS).

In the results published so far several contradictions can be discovered. All authors have observed a shift in the metal core level XPS lines toward higher binding energies with decreasing cluster size and a successive increase in the line width. In the transition metals where the density of states at the Fermi level is high (e.g., 3d peaks for Ni and Co), the intensity of 3d states strongly decreases with decreasing cluster size.^{1–3,16} On the contrary, for noble metals several authors have observed that

the Fermi edge and the whole valence band shifts toward higher binding energies with decreasing cluster size.^{3–5} On the other hand, others have measured significantly different shifts for the noble metal core level binding energy, d bands, and Fermi edges.^{6–9}

The changes described cannot be interpreted by uniform phenomena. They were—at least partly—attributed to the size-dependent changes in the electronic structure of the cluster,^{6,7,12} which results in the occurrence of a size-dependent metal-to-nonmetal transition in the smallest clusters.^{9–11} Others argued that these changes are due to the suppression of the screening of the metal core hole and to the appearance of a positive excess charge on the cluster during the time scale of photoemission.^{4,5} Recently, several papers have emphasized the role of the hybridization between the electronic states of the substrate and cluster.^{2,8,33}

However, from these data the real size correlation cannot be evaluated because the size distribution and shape of the particles deposited by thermal evaporation were hardly known. In addition to that, it was observed that at certain nucleation sites (mostly at surface steps) much larger clusters are grown than at other sites. These larger clusters may even form a one-dimensional chainlike structure¹⁸ which significantly differs from the assumed morphology consisting of evenly spaced isolated particles.

Recently, the interest is focused on free clusters in which the evolution of physical properties can be investigated,^{19,20} but these data can be correlated only to unsupported spherical particles.

[®] Abstract published in *Advance ACS Abstracts*, February 15, 1997.

A new possibility to create well-defined small particles is the laser ablation of a target material and subsequent sputtering of the film prepared. During laser ablation individual atoms, clusters, and larger particles are emitted from the target and deposited onto the substrate. Particle formation may be enhanced by cooling the ejected plasma by an inert gas atmosphere and scattering it on the gas atoms.¹⁷ These particles formed in the gas phase can be collected on a substrate on which the film formed consists of small particles. Isolated particles can be obtained by thinning the film by sputtering, and the size of the particles can also be decreased by this process. The sputtering process can be monitored by studying the electronic structure of the sample by means of ultraviolet photoelectron spectroscopy (UPS) and X-ray photoelectron spectroscopy (XPS). If the particle size in the beginning of the process is large enough to show bulk valence band density of states, the most size-dependent features of the valence band can be determined by this treatment. This seems to be an improved method compared to what was successfully applied for preparation of small cobalt particles from electron beam gun evaporated 5–10 nm thick discontinuous cobalt film.^{15,16}

The size dependence of the 3d and 4s states in transition metals has not been investigated separately and simultaneously. However, from these studies information can be obtained about the size dependence on localized and delocalized states of the valence band. Copper is a good candidate for this investigation as the 3d band is filled, and it appears at a binding energy higher than the Fermi level. On the other hand, the density of states at the Fermi level is *s* type.

The results of the XPS and UPS data measured on the small copper particles prepared by deposition of discontinuous film on amorphous carbon or graphite have been discussed.^{1,2,7,8,13} In these papers the observed decrease in the width of the 3d band is attributed to decreasing coordination number. The valence band binding energy shift is explained by rehybridization of *d* states to *s*-like states⁷ or hybridization between the cluster and the substrate surface originated states.^{2,8,33} The core level XPS line broadening and the shift are explained by both the reduction of metallic screening^{2,13} and valence band rehybridization.⁷ This is likely due to the reduction of the lattice constants in small particles.¹⁴

The main goal of the present paper is to obtain detailed information on the electronic structure of nonspherical, small copper particles deposited on a silicon substrate (Si(100)), that is, how the valence band and the core level structure of the delocalized and mainly localized electrons are altered during the transition from bulk state to small particles. The power of the preparation method by thinning by means of sputtering will also be demonstrated by a separate investigation on silver particles.

Experimental Section

Sample Preparation. P-type Si(100) wafers were cleaned in HF solution and were exposed to air for 2 weeks. This treatment leads to the formation of a not fully continuous and nonstoichiometric native oxide layer which is about 1 nm thick.²¹ Silicide formation is diminished by this layer in some cases,^{22,30} but in the case of nickel²³ and palladium²⁴ silicide formation is observed after high-temperature annealing by which the native oxide was destroyed. On the other hand, the thickness of native oxide is too low to cause charging problems. Although for copper the presence of native oxide makes the silicide formation unlikely, its possibility cannot be entirely omitted, and this point was separately investigated.

Copper film was deposited by laser ablation on these substrates in a vacuum chamber with base pressure better than

3×10^{-7} mbar. Silver films were deposited in the same way and used as a reference for small particle preparation because silver does not interact with silicon.⁶

A pulsed Nd–glass laser with 2 J pulse energy and 35 ns pulse length was applied for deposition. The targets were made of commercially available pure copper and silver. The layers were evaporated in 6 mbar of argon. The deposition of the films was monitored with a quartz crystal oscillator. Approximately 3–5 nm was the “equivalent thickness” of the films.

Experimental Techniques. In situ sputtering of the thin films and recording the photoelectron spectra were carried out in a KRATOS ES-300 photoelectron spectrometer. The films were thinned by sputtering with defocused Ar⁺ ions at energies of 1.5 keV (estimated ion flux 2×10^{13} ions/cm²s) with an angle of incidence of 60°. This arrangement ensured formation of isolated small copper particles and the continuous decreasing of the average size of the particles.

The X-ray photoelectron spectra (XPS) and ultraviolet photoelectron spectra (UPS) were recorded using Mg K α (1253.6 eV) and He I (21.2 eV) excitations, respectively, at different stages of sputtering to determine the size dependence of the electronic structure of copper particles. The pressure during the photoemission measurements was lower than 4×10^{-9} mbar.

The size and shape of the copper particles were determined by replica transmission electron microscopy with a JEOL 100U electron microscope before and after sputtering. The height of the particles was determined from their shadows on the replica. In order to check the replica results, the lateral geometry of the sputtered sample was also investigated by a Philips CM-20 transmission electron microscope after appropriate etching of the substrate. The silver sample was also investigated by lateral TEM at the end of the sputtering to check the sample preparation process.

Results and Discussion

Before describing the results on the electronic structure of the copper nanoparticles, the morphology studied by electron microscopy of the samples in the as-prepared state and after the sputtering process with 1.5 keV Ar⁺ ions is presented. In Figure 1a the morphology of the copper sample evaporated in 6 mbar of argon before sputtering (from now on it is denoted by “as-prepared”) is presented. The sample consists of particles with rather sharp lateral size distribution with a maximum at 80–100 nm. (Only the bright area in the middle of each “hill” belongs to the particle.) The height of the islands estimated from their shadows is about 10 nm (10% of their lateral size). There is a background between the particles which involves copper particles buried by a more or less continuous film. Several large particles can also be seen in the micrograph picture, but they originated from the replica preparation process.

The replica micrograph of the particles obtained on sputtered sample is presented in Figure 1b. It can be seen that after sputtering the background between the isolated particles disappeared, and this morphology indicates the appearance of cleaned and smooth silicon surface. From this observation it can be concluded that the morphology after the ion bombardment is not due to roughening of the substrate surface. It is well established that sputtering yield depends strongly on the angle of incidence of argon ions. This sputtering results in the formation of a rather flat, conical particle shape as demonstrated in a simulation of particle erosion by ion bombardment.²⁵ The lateral size of the structures obtained from the replica is typically in the 20–30 nm range; the much larger particles are artifacts due to the method of replica preparation.

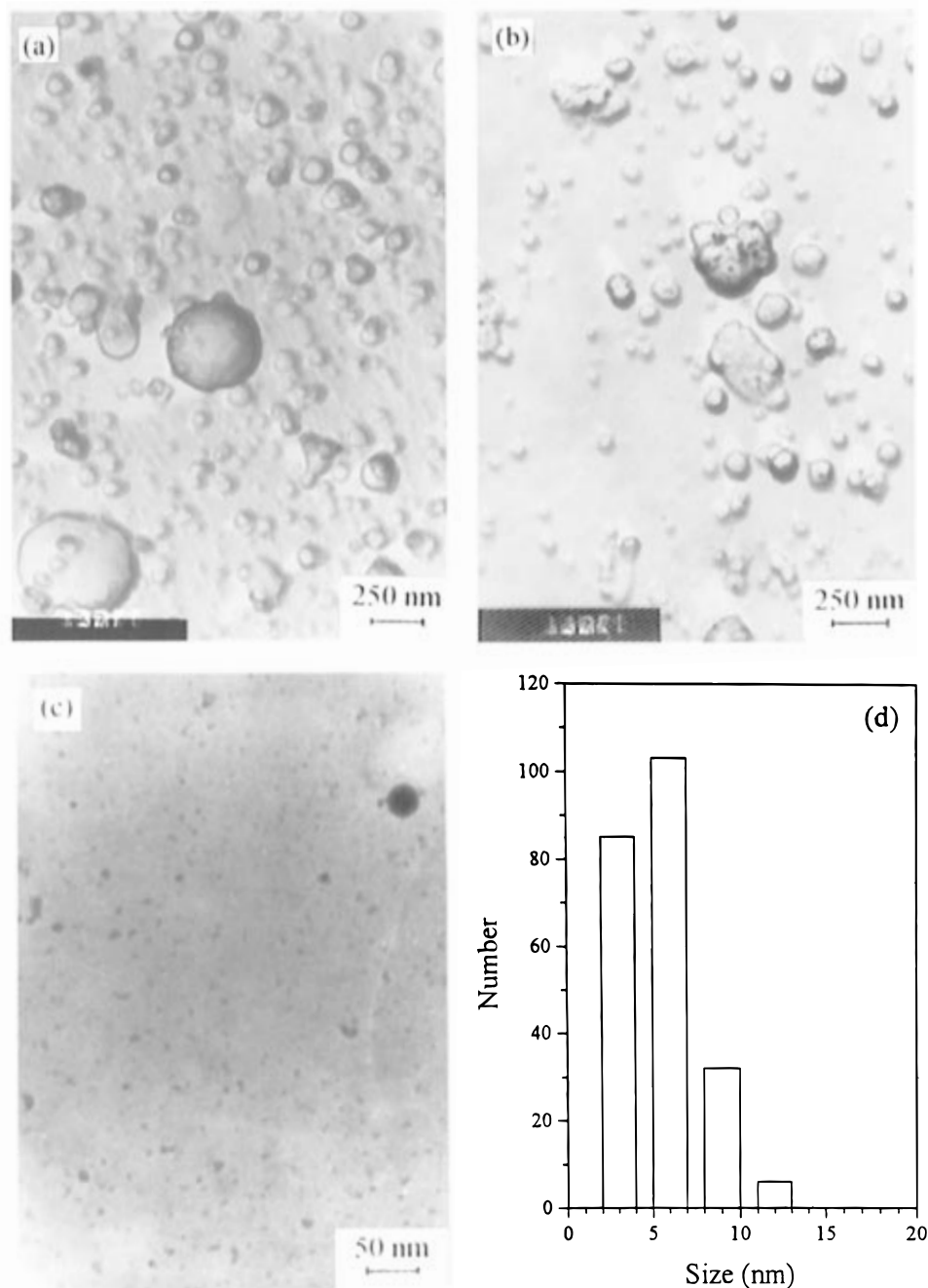


Figure 1. TEM micrographs of copper films deposited by laser ablation on Si(100) in 6 mbar of argon: (a) replica micrograph of the as-deposited sample; (b) replica micrograph at the end of sputtering, (c) lateral TEM micrograph at the end of the sputtering; (d) particle size distribution (from TEM micrograph picture c).

Evaluation of particle sizes from replica micrographs is not accurate enough and is good only for an estimation of the size range of the particles. This is partly due to the fact that the 10 nm size range is the lower limit of the lateral resolution of this method. Moreover, during sputtering a shadow of the original particles projected by the ion beam into the silicon substrate appears around the particles. The morphology caused by this shadow effect may not be distinguished from the remaining part of the copper particles, giving further uncertainties to the lateral size determination. On the other hand, the advantage of the replica method is that it does not need sample preparation which could disturb the particle distribution, and the available representative surface is not extremely low.

Owing to the limitations of the replica method, a lateral TEM investigation on the sputtered sample has been carried out. The result presented in Figure 1c indicates a rather sharp distribution in the particles size; more than 80% are in the range 3–6 nm

(Figure 1d). Since lateral transmission electron microscope picture is not affected by the projection effect mentioned, it can be concluded that replica method gives only a rough estimation for the upper limit of real particle sizes. However, the height of the particles cannot be obtained from lateral TEM measurements. Nevertheless, the height of the particles formed after sputtering can be estimated to be around 2–3 nm using the replica micrographs, which means that the typical particle shape is different from spherical.

Si 2p and O 1s emissions in Figure 2a,b are indicative of the presence of native silicon oxide. The main Si 2p peak at 99.8 eV does not change its position during sputtering. According to the literature data, a component with a chemical shift of 3.4 eV in the Si 2p line (at 103.2 eV) indicates a 1–2 nm thick SiO_{2-x} surface layer²⁶ at the beginning the sputtering process. The binding energy of the O 1s line (532.5 eV) is characteristic of SiO_2 . After sputtering, the silicon is still not completely clean

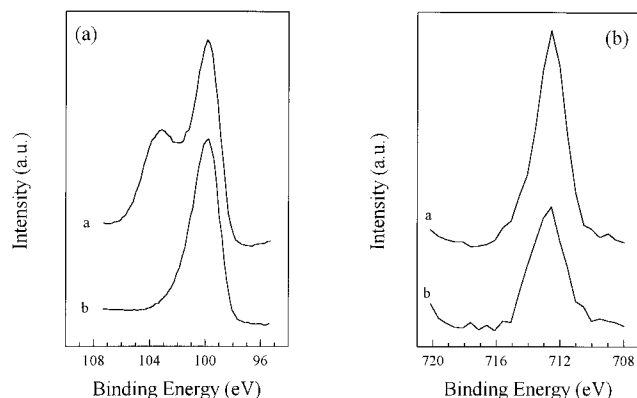


Figure 2. (a) Si 2p and (b) O 1s core level XPS spectra of the Si(100) substrate of the copper sample evaporated in 6 mbar of argon: (a) after cleaning for 8 min by sputtering; (b) after sputtering for 81 min.

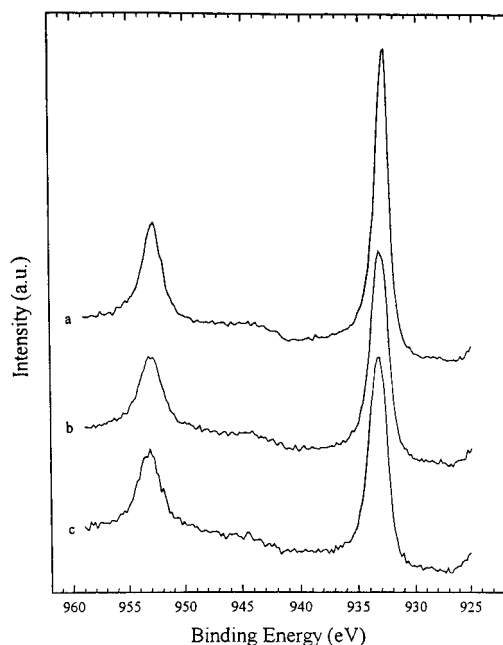


Figure 3. Cu 2p core level XPS spectra of copper on Si(100) sample evaporated in 6 mbar of argon: (a) after cleaning for 8 min by sputtering; (b) after sputtering for 38 min; (c) after sputtering for 81 min.

TABLE 1: Characteristics of Cu 2p_{3/2} Line at the Beginning and End of the Sputtering for the Copper Sample Deposited in 6 mbar of Argon

treatment	binding energy (eV) (error: 0.1 eV)	full width at half-maximum (eV) (error: 0.2 eV)
8 min sputtering	932.8	1.4
81 min sputtering	933.2	1.8

as indicated by the asymmetry of the 2p line. This is further supported by the significant O 1s emission at 532.3 eV, which indicates a SiO_x layer.

In Figure 3 the Cu 2p core level spectra of the sample in the beginning of the sputtering (curve a), at an intermediate stage (curve b), and after sputtering for 81 min (curve c) can be seen. The Cu 2p core levels gradually shifted from the value characteristic of the bulk (932.8 eV) toward higher binding energies (933.2 eV), measured with a precision of ± 0.1 eV. Broadening of the peaks is also obviously observable, and the measured binding energies and peak widths are presented in Table 1. The fwhm value for Cu 2p_{3/2} changes from 1.4 ± 0.2 to 1.8 ± 0.2 eV and that for Cu 2p_{1/2} from 2.0 ± 0.2 to 2.4 ± 0.2 eV. The Auger LMM lines also shifted toward higher

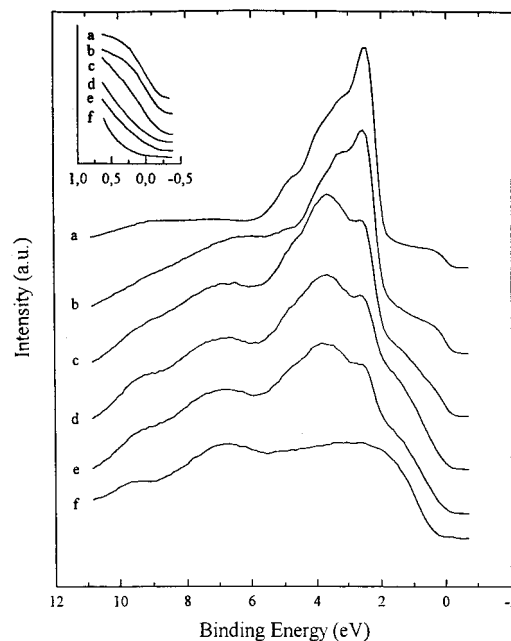


Figure 4. Valence band UPS spectra of the copper sample evaporated in 6 mbar of argon: (a) clean bulk copper, for comparison; (b)–(e) after 8, 23, 43, 58, and 81 min sputtering, respectively; (f) Si(100) single crystal used as a reference after sputtering for 30 min. Insert: emission from the region of the Fermi energy for the same spectra.

binding energies with the same value as the Cu 2p core levels. The observed shifts in binding energies are in agreement with those observed for copper clusters by other authors.^{2,7,8}

In Figure 4 He I excited valence band UPS spectra of the Cu/Si(100) sample are shown. Curve a represents a clean bulk copper spectrum, while curve f is recorded on a sputtered silicon surface, and both are given for the sake of comparison. There are three main regions in the spectra of the copper layers. The first one is at the Fermi level (at around 0 eV binding energy) which represents Cu 4s states. The second one (between 2 and 5 eV binding energies) arises from Cu 3d states. The third one is a broad peak at about 7 eV which results from oxygen 2p states. This peak is due to the nonremoved fraction of the silicon oxide barrier layer between copper and silicon. The presence of the sharp Cu 3d peak at 2.5 eV binding energy shows clearly that copper is not oxidized and/or contaminated at all. During sputtering the spectral region at around 7 eV becomes similar to the same region of the spectrum of the sputtered silicon (curve f). On the other hand, in the Cu 3d band important changes take place during sputtering. The first peak at 2.5 eV significantly decreases, but its position remains unchanged. This remaining small peak maybe correlated to larger (bulklike) particles.

During decreasing the copper particles' size a new peak appears in the valence band spectra which originates from the shoulder of the bulk Cu 3d spectrum located at about 3.6 eV. The peak shifts toward higher binding energies (to 3.8 eV) toward the end of sputtering. The variation of the binding energy of this higher binding energy peak during sputtering is presented in Table 2. Near the Fermi level the emission becomes rather silicon-like (from curve c); the metallic Fermi edge is invisible by photoemission after the sputtering (curve e, see also insert). The small peak at 9.5 eV is due to 3p states of argon atoms embedded into the substrate.

XPS measurement gives similar shift for the size reduction of the small copper particles. Due to its limited resolution, XPS gives a single broad peak even for the bulk Cu 3d band, the centroid of which shifts by 0.5 eV toward higher binding

TABLE 2: Binding Energy of the Maximum of the Cu 3d Band after Different Treatments As Measured by UPS

treatment	binding energy (eV)	comment
23 min sputtering	3.6	from Figure 4c
58 min sputtering	3.6	from Figure 4d
81 min sputtering	3.8	from Figure 4e
annealing of vacuum evaporated Cu film at 300 °C for 30 min	3.5	Cu silicide, from Figure 6b

energies during sputtering. The binding energy values are presented in Table 3. The peak is narrower by 0.1–0.2 eV at the end of the sputtering. These values are similar to those reported by others.^{7,8} However, from the UPS spectra one could see that the change in the valence band involves not only a simple narrowing and shift of the copper peak but also a strong reduction of the first 3d peak at 2.5 eV binding energy (Figure 4). This decrease gives an apparent contribution to the band narrowing and shift because of the limited resolution of XPS.

From the observed changes one may conclude that the most size-sensitive part of the valence band is the 3d peak at 2.5 eV binding energy; i.e., it gradually disappears during size reduction. Further reducing the size, the remaining part of the valence band shifts toward higher binding energies, and the density of states begins to decrease on the Fermi level.

In order to support our finding on small copper particles, the valence band properties of the similarly prepared small silver particles were investigated. Figure 5 shows the XPS valence band spectra of the silver sample at different stages of the sputtering. The spectra are presented after subtraction of substrate curve. Curve a is the valence band of bulk silver and is given for comparison. The silver 4d doublet is not fully resolved even for bulk silver because of the limited resolution of XPS. It can be seen in the spectra that during sputtering first the Ag 4d peak located at 4.8 eV begins to decrease and then the maximum of the remaining part of the 4d band shifts toward higher binding energies by 1.1 eV and its width decreases by 0.7 eV at the end of sputtering. The core levels and the Auger lines were also shifted by 0.4 eV at the end of sputtering. From TEM measurements the typical lateral particle size was about 5 nm after sputtering. Since changes in the electronic structure are essentially the same as described in the literature, where a shift of the valence band centroid of 0.6–0.8 eV and a decrease of its width by 0.8–1 eV with respect to bulk value were reported for small silver particles with sizes of a few nanometers,^{3,6} one can conclude that it is possible to prepare well-defined small particles by laser evaporation in an inert gas atmosphere and subsequent low-energy ion bombardment.

As beneath the copper particles there exists a rather thin, more or less discontinuous and nonstoichiometric native silicon oxide layer, this cannot be an electrical insulator that should be necessary for electrostatic charging effects or formation of contact potentials. The shift in the valence band and in the core level energies is continuous during sputtering; thus, one may expect the presence of small particles with decreasing size. Furthermore, the band bending at the Fermi level makes uncertainty only in the energy level of the silicon substrate and does not affect the energy scale for the metal.²⁷ Consequently, the shifts due to the charging effects and/or to the band bending at Fermi level can be excluded. Moreover, the sputtering-induced modification in the shape of the copper valence band cannot be explained by charging, either. However, oxidation of the copper particles and copper silicide formation could cause other artifacts. It is, therefore, a prerequisite to prove the lack of occurrence of these phenomena.

The presence of CuO can be ruled out on the basis of the Cu 2p core level spectra (Figure 3) because the core levels of copper

in CuO are much broader than in the bulk copper; they shift toward higher binding energies with a much larger value than the small particles (with 1 eV) with respect to the bulk and show strong satellite structure.²⁸ The shape of XPS and UPS valence band spectra of Cu₂O is substantially different from our spectra.²⁸ Moreover, the core levels and Auger lines shift in a parallel manner, which means that the Auger parameter remains constant, close to its bulk value.²⁶ Since this parameter is especially sensitive for the changes of the chemical state, this result further supports the conclusion that the observed changes cannot be explained by oxidation of the copper.

In order to study the effect of copper–silicon interaction on the valence band spectra, the copper was evaporated on a clean silicon surface and annealed at 300 °C for 30 min. This treatment may serve as a model for copper diffusion into the silicon substrate, i.e., formation of copper silicide (mainly Cu₃Si), and also for intermixing caused by the 1.5 keV Ar⁺ ion bombardment. The UPS valence band spectra of these samples are shown in Figure 6. The changes in the valence band emission due to the heat treatment involve the shift of the 3d band toward higher binding energies and the complete disappearance of the lower binding energy 3d peak. However, the 3d band in the annealed or intermixed sample is located at a binding energy which is 0.2–0.3 eV lower than that of the spectra recorded for small particles (compare the data in Tables 2 and 3). Moreover, the shape of the valence band is more symmetrical than that measured for small particles (compare curve e of Figure 4 and curve b of Figure 6). In addition, the most important feature is the Fermi edge that remains visible after the heat treatment (Figure 6, see insert).

Our results on the heat-treated copper–silicon are similar to that obtained for intermixed copper–silicon system by depositing a small amount of copper on a very clean silicon surface^{29–31} and for Cu₃Si.²⁹ According to these data, the copper core level binding energies shifting toward higher values (with 0.5–0.6 eV^{29–31}) are similar but not identical to the value observed for small particles. The shift in the maximum of the valence band were observed to be about 1 eV,²⁹ which leads to a peak located at 3.5 eV binding energy as measured by UPS.³¹

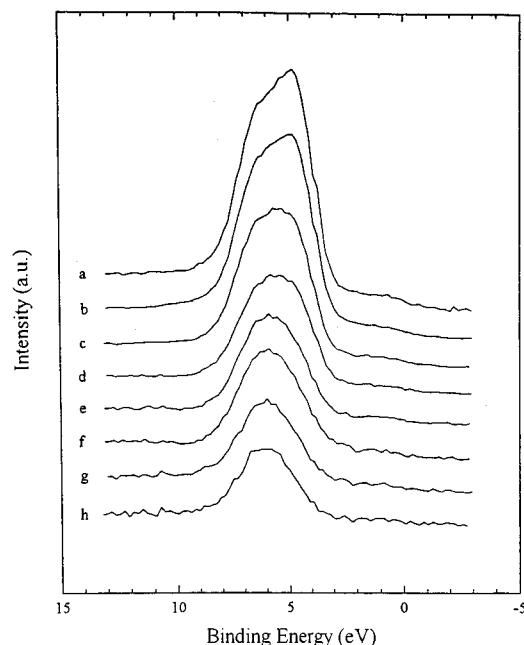
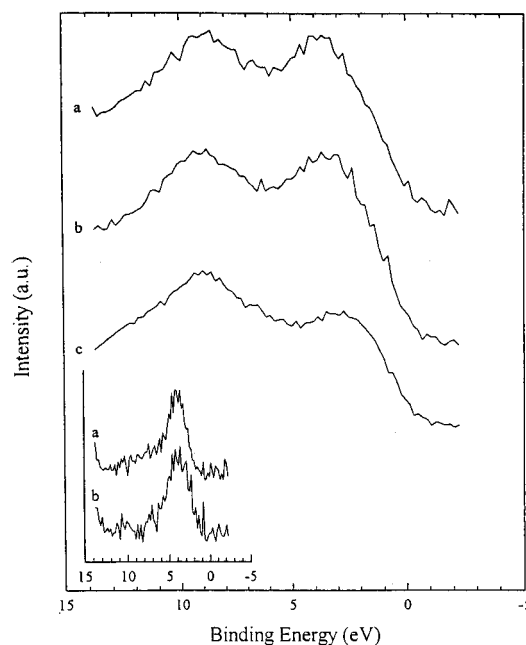
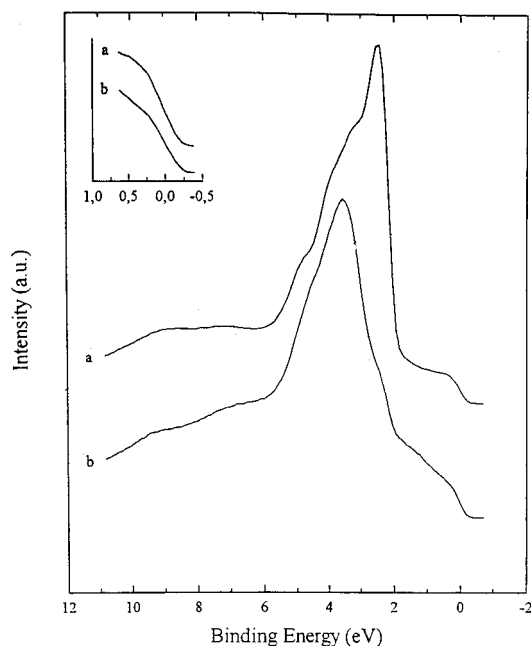
Since the valence band of the annealed or intermixed system significantly differs from the valence band observed on our samples containing small particles, the characteristics of the sputtered island film cannot be explained by intermixing or silicide formation.

This conclusion is further supported by the observation of the changes in the valence band induced by heat treatment of the small particles at the end of sputtering. Here this treatment gives a possibility to exclude the sputtering induced silicide formation in the small copper particles. If the particles were of copper silicide instead of pure copper, annealing at relatively low temperature (200–300 °C) should not induce any changes because the silicon–copper reaction is already fulfilled during sputtering. Furthermore, the copper atom in copper silicide does not have a large diffusion coefficient in silicon in contrast to pure copper; thus, diffusion into the silicon substrate should be limited, which means that copper concentration at the surface should not decrease.

Following this suggestion we measured the effect of in situ heat treatment on the valence band of the sputtered small copper particle–silicon substrate system. The XPS valence band spectra are presented in Figure 7. Here curve a shows the valence band of the sputtered small particles, while curve b represents the same sample after annealing at 30 min for 250 °C and short cleaning with Ar⁺ ion bombardment. Curve c shows XPS valence band spectrum of the clean silicon substrate

TABLE 3: Binding Energy of the Maximum of the Cu 3d Band after Different Treatments As Measured by XPS

treatment	binding energy (eV)	comment
8 min sputtering	3.5	from Figure 4
38 min sputtering	3.8	from Figure 4
81 min sputtering	4.0	from Figure 4
annealing of a vacuum-deposited Cu film at 300 °C	3.8	Cu silicide
extended sputtering in order to obtain small particles	4.05	small particles (from Figure 7)
annealing of small particles at 250 °C for 30 min	3.8	annealed small particles forming Cu silicide (from Figure 7)

**Figure 5.** Valence band XPS spectra of silver deposited on Si(100) surface in 6 mbar of argon: (a) bulk metallic silver; (b)–(f) after sputtering Ag/Si(100) or 2, 7, 10, 30, 33, 39, and 42 min, respectively, by Ar⁺ ion sputtering.**Figure 7.** Valence band XPS spectra of small copper particles formed on the Si(100) substrate before annealing (a) and after heat treatment at 250 °C for 30 min followed by 2 min sputtering (b). (c) Spectrum of sputtered Si(100) for comparison. Insert: the same as (a) and (b), after removing the substrate contribution.**Figure 6.** Valence band UPS spectra of copper sample evaporated in vacuum: (a) after 10 min sputtering; (b) after annealing at 300 °C for 30 min followed by 31 min sputtering. Insert: emission from the region of the Fermi energy for the same spectra.

after sputtering. It can be seen that the 3d peak is shifted by 0.3 eV toward lower binding energy, and the line width is larger in the annealed sample. The position of the peak is similar to the that of the valence band peak of Cu₃Si.

It is seen that annealing causes definite change in the 3d states mainly by new states appeared at lower binding energy in the region in which copper silicide originated states were observed. In addition to that, a decrease of Cu 2p/Si 2p ratio was observed during the heat treatment, which suggests that a certain fraction of the copper atoms diffused into the substrate during heat treatment. Consequently, copper silicide formation was initiated unambiguously by thermal treatment. Thus, the small particles consist of pure copper and not of copper silicide.

In conclusion, the changes of the valence band density of states observed during reducing of the particle size by sputtering cannot be attributed to chemical interaction with the substrate. This is further supported by our experiments performed on silver particles deposited on silicon, where similar changes of the electronic structure were observed (see Figures 4 and 5), although silver is known not to interact with silicon at all.⁶ Similarly, silicide formation in the Co/Si(100) system under the same conditions that were applied here did not occur.^{15,16}

It should be mentioned that in spherical clusters the strong differences between the electronic structures representing the bulk and clusters occur only if the clusters consists of fewer than 300 atoms.²⁰ In contrast, in the “raftlike structure” of our particles when one dimension is 2–3 times smaller than the other, size-dependent changes in the electronic structure appear in systems containing several thousand atoms. Nevertheless, it can be due to some size-dependent nonchemical interaction between the copper particles and the substrate as suggested in refs 2, 8, and 33. But since we did not find signs of such an interaction on the substrate core levels, in our opinion this result is—at least partly—explained by a shape-dependent behavior of

the valence band density of states since the shape of the sputtered nanoparticles significantly differs from spherical ones. This assumption is supported by the results of Haruta et al. obtained for small gold particles which show that the catalytic properties are affected by the shape of the particles.³²

Conclusion

By the laser ablation and sputtering islandlike, isolated nonspherical copper particles in the 2–3 nm range for height and around 3–6 nm range for lateral dimensions are formed. The rearrangement of the electronic states was unambiguously detected during sputtering, and it is related to the size effect excluding any other effects such as chemical interactions. The Cu 2p core level and the Auger lines shifted toward higher binding energy by 0.3 eV, in agreement with other published data. The valence band density of states for the copper particles is characterized by the strong decrease of 3d states at the binding energy of 2.5 eV while the density of states at higher binding energy only slightly shifts toward higher values. Further reducing the size, the density of states at the Fermi level strongly decreases at least at the sensitivity of the photoemission (UPS, XPS). Thus, the most size-sensitive valence states are the 3d states located at low binding energy.

Acknowledgment. The authors are indebted to the National Science and Research Fund for financial support (Grants 2963 and 7213) and to K. N. Tu for valuable discussions.

References and Notes

- (1) Egelhoff, W. F.; Tibbets, G. G. *Phys. Rev. B* **1979**, *19*, 5028.
- (2) Vijayakrishnan, V.; Rao, C. N. R. *Surf. Sci.* **1991**, *255*, L516.
- (3) Wertheim, G. K.; DiCenzo, S. B.; Buchanan, D. N. E. *Phys. Rev. B* **1986**, *33*, 5384.
- (4) Wertheim, G. K.; DiCenzo, S. B. *Phys. Rev. B* **1985**, *37*, 844.
- (5) Wertheim, G. K.; DiCenzo, S. B.; Youngquist, S. E. *Phys. Rev. Lett.* **1983**, *51*, 2310.
- (6) Pennisi, A. R.; Costanzo, E.; Faraci, G.; Hwu, Y.; Margaritondo, G. *Phys. Lett. A* **1992**, *169*, 87.

- (7) DeCrescenzi, M.; Diociaiuti, M.; Lozzi, L.; Picozzi, P.; Santucci, S. *Solid State Commun.* **1990**, *74*, 115.
- (8) DiNardo, S.; Lozzi, L.; Passacantando, M.; Picozzi, P.; Santucci, S.; DeCrescenzi, M. *Surf. Sci.* **1994**, *307–308*, 922.
- (9) Vijayakrishnan, V.; Chainani, A.; Sarma, D. D.; Rao, C. N. R. *J. Phys. Chem.* **1992**, *96*, 879.
- (10) Rao, C. N. R.; Vijayakrishnan, V.; Aiyer, H. N.; Kulkarni, G. U.; Subbanna, G. N. *J. Phys. Chem.* **1993**, *97*, 11157.
- (11) Aiyer, H. N.; Vijayakrishnan, V.; Subbanna, G. N.; Rao, C. N. R. *Surf. Sci.* **1992**, *313*, 392.
- (12) Mason, M. G. *Phys. Rev. B* **1983**, *27*, 748.
- (13) Jirka, I. *Surf. Sci.* **1990**, *232*, 307.
- (14) Gautier, M.; Pham Van, L.; Durand, J. P. *Europhys. Lett.* **1992**, *18*, 175.
- (15) Bogdányi, G.; Zsoldos, Z.; Pető, G.; Gucci, L. *Surf. Sci.* **1994**, *306*, L563.
- (16) Pető, G.; Bogdányi, G.; Molnár, G.; Gucci, L. *Catal. Lett.* **1994**, *26*, 383.
- (17) Faust, P.; Brandstaettner, M.; Ding, A. Z. *Phys. D* **1991**, *21*, 286.
- (18) Francis, G. M.; Kuipers, L.; Cleaver, J. R. A.; Palmer, R. E. *J. Appl. Phys.* **1996**, *79*, 2942.
- (19) de Heer, W. A. *Rev. Mod. Phys.* **1993**, *65*, 611.
- (20) Taylor, K. J.; Pettiette-Hall, C. L.; Chesnovsky, O.; Smalley, R. E. *J. Chem. Phys.* **1992**, *96*, 3319.
- (21) Graf, D.; Grunder, M.; Schulz, R.; Mühlhof, L. *J. Appl. Phys.* **1990**, *68*, 5155.
- (22) Liehr, M.; LeGoues, F. K.; Rubloff, G. W.; Ho, P. S. *J. Vac. Sci. Technol.* **1985**, *A3*, 984.
- (23) Sarapatka, T. J. *J. Electron Spectrosc.* **1993**, *62*, 335.
- (24) Schleich, B.; Schmeisser, D.; Göpel, W. *Surf. Sci.* **1987**, *191*, 367.
- (25) Sakamoto, T.; Tomiyasu, B.; Owari, M.; Nihei, Y. *Surf. Interface Anal.*, in press.
- (26) Moulder, J. F.; Stickle, W. F.; Sobol, P. E.; Bomben, K. D. In *PHI Handbook of Photoelectron Spectroscopy*; Chastain, J., Ed.; Perkin-Elmer Corp. Physical Electronics Division: Eden Prairie, MN, 1992.
- (27) Horn, K.; Alonso, M.; Cimino, R. *Appl. Surf. Sci.* **1992**, *56–58*, 271.
- (28) Ghijsen, J.; Tjeng, L. H.; van Elp, J.; Eskes, H.; Westerink, J.; Sawatzky, G. A.; Czyzyk, M. T. *Phys. Rev. B* **1988**, *38*, 11322.
- (29) Cros, A.; Aboelfotoh, M. O.; Tu, K. N. *J. Appl. Phys.* **1990**, *67*, 3328.
- (30) Corn, S. H.; Falconer, J. L.; Czanderna, A. W. *J. Vac. Sci. Technol.* **1988**, *A6*, 1012.
- (31) Ringeisen, F.; Derrien, J.; Daugy, E.; Layet, J. M.; Mathiez, P.; Salvan, F. *J. Vac. Sci. Technol.* **1983**, *B1*, 546.
- (32) Sakurai, H.; Haruta, M. *Catal. Today* **1996**, *29*, 361.
- (33) Mason, M. G.; Baetzold, R. C. *J. Chem. Phys.* **1976**, *64*, 271.